RARE METALS
Vol. 31, No. 5, Oct. 2012, p. 474
DOI: 10.1007/s12598-012-0542-3

Synthesis and electrochemical performance of $LiMnPO_4$/C composites cathode materials

ZHONG Shengkui[a, b], XU Yuebin[a], LI Yanhong[a, b], ZENG Honghu[a, b], LI Wei[a], and WANG Jian[a]

[a] *College of Environmental Science and Engineering, Guilin University of Technology, Guilin 541004, China*
[b] *Guangxi Key Laboratory of Environmental Engineering, Protection and Assessment, Guilin University of Technology, Guilin 541004, China*

Received 18 November 2011; received in revised form 22 February 2012; accepted 21 March 2012

Abstract

$LiMnPO_4$/C composites were synthesized via solid-state reaction with different carbon sources: sucrose, citric acid and oxalic acid. The samples were characterized by X-ray diffraction (XRD), scanning electron microscopy (SEM) and electrochemical performance test. The results of XRD reveal that carbon coating has no effect on the phase of $LiMnPO_4$. The $LiMnPO_4$/C synthesized at 600 °C with citric acid as carbon source shows an initial discharge capacity of 117.8 $mAh \cdot g^{-1}$ at 0.05 C rate. After 30 cycles, the capacity remains 98.2 $mAh \cdot g^{-1}$. The improved electrochemical properties of $LiMnPO_4$/C is attributed to the decomposition of organic acid during the sintering process.

Keywords: lithium-ion battery; cathode material; carbon coating; $LiMnPO_4$

1 Introduction

The olivine $LiMnPO_4$ is promised to be the potential cathode material for rechargeable lithium ion battery, which shows only one-dimensional channel for significant lithium ion diffusion [1−3]. The $LiMnPO_4$ shows a voltage platform of 4.1 V, much higher than $LiFePO_4$. However, the large rate charge-discharge capacity is significantly low [4], so the application of $LiMnPO_4$ is limited. The poor conductivity of electrodes is mostly due to the difficulty in lithium ion diffusion. The structure defects in the $LiMnPO_4$ cause the difficulty in lithium ion diffusion. Because of blockages in one-dimensional and three-dimensional channels, lithium ions can only diffuse around the blocked sites [5]. The key rate-limiting factor is suggested to be the high effective mass of polarons, because of the Jahn-Teller effect around an Mn^{3+}-ion[4]. However, the disputed problems are the existence of olivine $MnPO_4$ and the electrochemical delithiation properties of $LiMnPO_4$/$MnPO_4$ phase [6−7]. Efforts to improve conductivity of $LiMnPO_4$ are concentrated on particle diameter optimization [6−8], carbon coating [9−11], and metal cation doping [12−14]. The carbon coating is regarded as the fairly effective and convenient route to improve the conductivity of $LiMnPO_4$. The organic acid as carbon source is adopted for coating. Because of the decomposition effect in the sintering process, the optimal particle size of $LiMnPO_4$ can be obtained. As a result, the length of lithium ion diffusion is reduced [15−17] and the reversible lithiation-delithiation can perform well.

In this paper, $LiMnPO_4$/C composites were synthesized via a solid-state reaction, using sucrose, citric acid and oxalic acid as carbon sources. All these carbon sources belonged to the organic acid. During the sintering process, organic acid was broken down. Also, the carbon resulting from thermal decomposition attached to the particle surface of $LiMnPO_4$/C, which could improve the conductivity. Then the effects of these carbon sources on the properties of $LiMnPO_4$/C were investigated.

2 Experimental

$LiMnPO_4$/C composites were synthesized by a solid-state reaction method. $MnCO_3$, Li_2CO_3, $NH_4H_2PO_4$ and carbon sources (sucrose, citric acid and oxalic acid) with a stoichiometric ratio were mixed homogeneously in an alcohol medium with ball-milling. The mixture removed to the vacuum drying oven was dried at 60 °C for 10 h. As a final step, the mixture was sintered at 500~700 °C for 20 h under argon atmosphere.

Powder X-ray diffraction (XRD, X`Pert Pro) using

Corresponding author: LI Yanhong **E-mail:** lyh1685@163.com

Cu-Kα radiation over the 2θ range of 10°~80° with a step size of 0.02° was employed to identify the crystalline phase of the synthesized materials. The particle morphologies of the powders were observed using scanning electron microscopy (SEM, JSM-6380LV). The electrochemical characterizations were performed using CR2025 coin-type cells. For positive electrodes fabrication, the prepared active material $LiMnPO_4$ was mixed with 10 wt.% of carbon black and 10 wt.% of polyvinylidene fluoride in N-methyl pyrrolidinone until slurry was obtained. And then the blended slurries were pasted onto an aluminum current collector, and the electrode was dried at 120 °C for 4 h in vacuum. The cathodes were punched into circular discs with a diameter of 1.2 cm. The test cells consisted of the positive electrode and lithium foil negative electrode separated by a porous polypropylene film, and 1 mol·L^{-1} $LiPF_6$ in EC: EMC: DMC (1:1:1 in volume) as the electrolyte. The assembly of the cells was carried out in a dry Ar-filled glove box. The cells were charged and discharged over a voltage range of 2.75 to 4.50 V versus Li/Li^+ electrode on battery testers (BTS-5V3A) at 0.05 C rate. The cyclic voltammogram (CV) and electronic impedance spectroscopy (EIS) were investigated by electrochemical workstation (CHI660A). The CV was tested at a scanning rate of 0.1 mV·s^{-1} in the voltage range of 2.5~4.5 V. The EIS were performed at 5 mV from 10 kHz to 10 mHz.

3 Results and discussion

The precursor with citric acid as carbon source was sintered at temperatures ranging from 500 to 700 °C for 20 h. Figure 1 compares the XRD patterns of $LiMnPO_4$/C samples sintered at different temperatures. The amount of carbon in the $LiMnPO_4$/C is about 3.1 wt.% determined by C-S analysis method. No evidence of diffraction peaks for crystalline carbon (graphite) appears in the diffraction pattern, which indicates that the carbon generated from citric acid is amorphous carbon and its presence does not influence the structure. All the characteristic peaks of three samples could be indexed as orthorhombic olivine $LiMnPO_4$. As the temperature increases, the intensity of the diffraction peaks is obviously strengthened. Therefore, the optimal crystallinity of $LiMnPO_4$/C can be obtained because of the appropriate high calcination temperature.

Further efforts are made to investigate the effect of different carbon sources on $LiMnPO_4$/C. Figure 2 shows the XRD patterns of $LiMnPO_4$/C samples synthesized at 600 °C with sucrose, citric acid and oxalic acid as carbon sources. The peaks of $LiMnPO_4$/C samples with different carbon sources are entirely identical, and no impurities peaks could be found in the patterns. Therefore, all carbon sources transform into amorphous carbon, distributing in the samples. It shows that all $LiMnPO_4$/C composites have the same olivine structure and a space group of Pmnb as pure $LiMnPO_4$. Thus, it is clear that different carbon sources coating has no effects on the phase of $LiMnPO_4$.

The SEM of the $LiMnPO_4$/C samples with citric acid was used to evaluate the effect of different sintering temperatures on the surface morphology. Figure 3 shows the microstructure of $LiMnPO_4$/C powders with citric acid sintered at temperatures ranging from 500 to 700 °C for 20 h. At 500 °C, the particle size of $LiMnPO_4$/C is so irregular that the lithium diffusion gets embarrassment. It is attributed to that the lower sintering temperature is adverse to obtain the uniform particle of $LiMnPO_4$/C. However, the particle diameter is well-distributed at 600 °C, and spherical particles can be observed in Fig. 3(b). However, the particle sizes become larger as the sintering temperature rises to 700 °C. Serious agglomeration in Fig. 3(c) will make a poor electro-

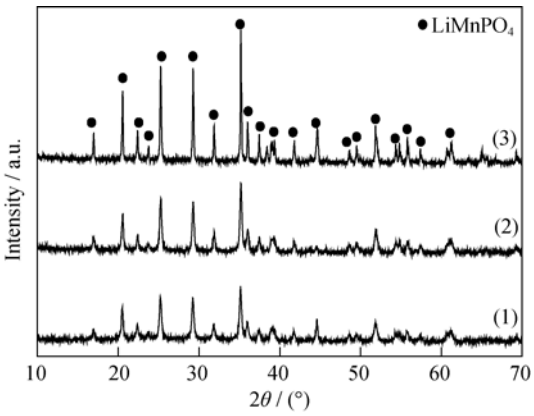

Fig. 1 X-ray diffraction patterns of $LiMnPO_4$/C samples sintered at different temperatures
(1) 500 °C; (2) 600 °C; (3) 700 °C

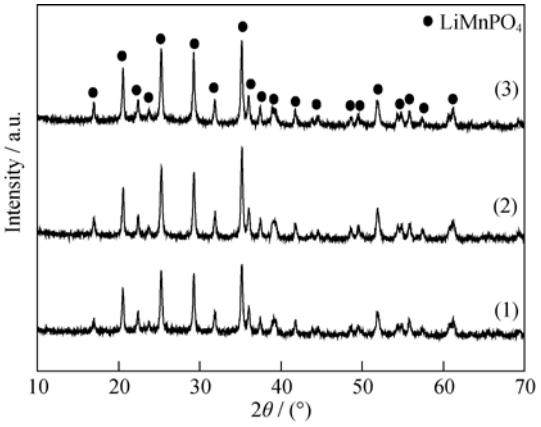

Fig. 2 X-ray diffraction patterns of $LiMnPO_4$/C samples synthesized with different carbon sources
(1) Oxalic acid; (2) Citric acid; (3) Sucrose

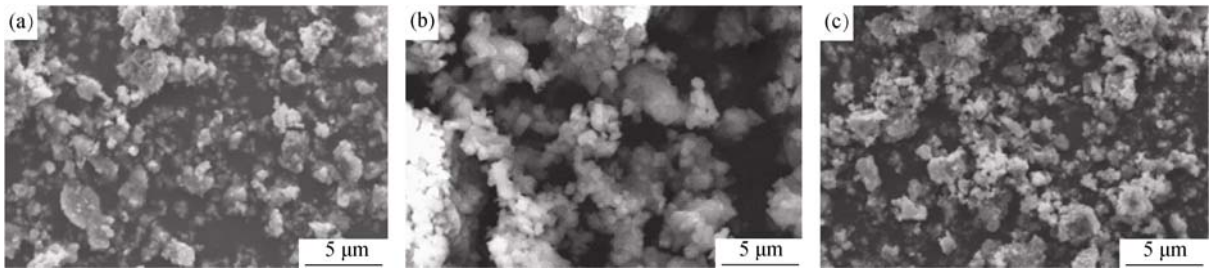

Fig. 3 SEM images of $LiMnPO_4$/C samples sintered at different temperatures
(a) 500 °C; (b) 600 °C; (c) 700 °C

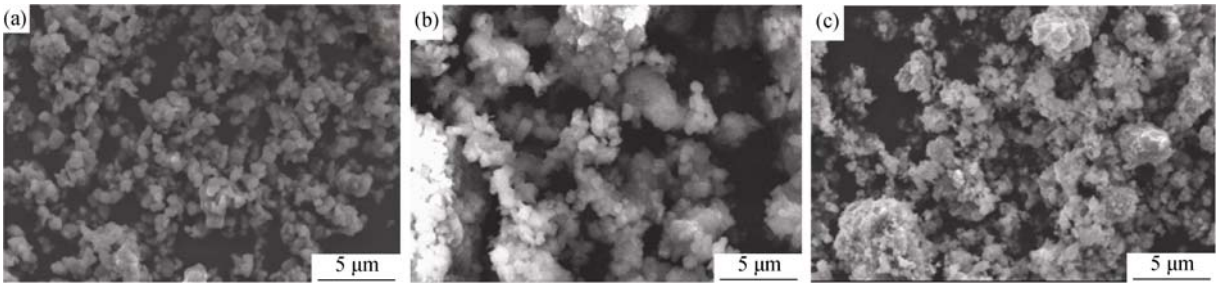

Fig. 4 SEM images of $LiMnPO_4$/C samples synthesized with different carbon sources
(a) Oxalic acid; (b) Citric acid; (c) Sucrose

chemical performance of this sample. Thus, the well-distributed particle of $LiMnPO_4$/C could be obtained at 600 °C.

The SEM images of $LiMnPO_4$/C samples prepared with different carbon sources are shown in Fig. 4. It illustrates the irregular particle sizes of $LiMnPO_4$/C with oxalic acid in Fig. 4(a). The sample using sucrose as carbon source is observed to have serious agglomeration in Fig. 4(c). On the contrary, citric acid as carbon source can be used to form the fairly homogeneous particles, which are illustrated in Fig. 4(b). It is considered that the decomposition effect of organic acid during the sintering process is favorable to control the particle size and prevent the agglomeration. Meanwhile, this decomposition effect of organic acid can generate carbon monoxide that is attributed to maintaining the stability of Mn^{2+} in the sintering process. Thus, the distance of lithium ion diffusion is shortened, which is favorable to modify the lithiation-delithiation process.

The electrochemical performance of $LiMnPO_4$/C was characterized by a charge-discharge test at the rate of 0.05C. This sample exhibits a reversible plateau around 4.1 V vs. Li/Li^+, which is the typical redox potential of Mn(II)↔ Mn(III) in the $LiMnPO_4$ system. The $LiMnPO_4$/C samples with citric acid as carbon source demonstrate a reversible initial discharge capacity of 105 $mAh·g^{-1}$ at 500 °C, 117.8 $mAh·g^{-1}$ at 600 °C and 107.2 $mAh·g^{-1}$ at 700 °C, as examined in Fig. 5. The cycling results of three samples are shown in Fig. 6. After 30 cycles, it retained 98.2 $mAh·g^{-1}$ at 600 °C. The capacity of two other samples synthesized at 500 °C and 700 °C reduced so rapidly, which retained 76.9 $mAh·g^{-1}$ and 81.1 $mAh·g^{-1}$ after 30 cycles. In a word, the good electrochemical performance is obtained, when the $LiMnPO_4$/C powders with citric acid are sintered at 600 °C.

The first discharge curves of $LiMnPO_4$/C samples are illustrated in Fig. 7 and the results of cycling performance are shown in Fig. 8. The curves present that the good charge-discharge performance is obtained with citric acid as carbon source, with the initial discharge capacity of 117.8 $mAg·h^{-1}$ and residual capacity of 98.2 $mAh·g^{-1}$ after 30 cycles. The electrochemical performance of $LiMnPO_4$/C with oxalic acid is close to the former, with the initial discharge capacity of 114.8 $mAg·h^{-1}$ and residual capacity of 92.4 $mAh·g^{-1}$ after 30 cycles. However, the first discharge capacity of the sample with sucrose is 110.6 $mAh·g^{-1}$, retaining 89.7 $mAh·g^{-1}$ over 30 cycles.

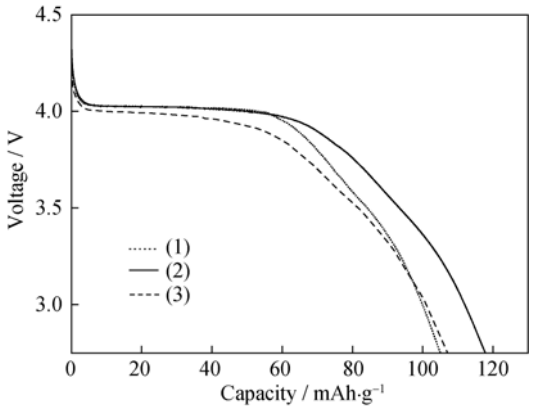

Fig. 5 Initial discharge curves of $LiMnPO_4$/C samples sintered at different temperatures
(1) 500 °C; (2) 600 °C; (3) 700 °C

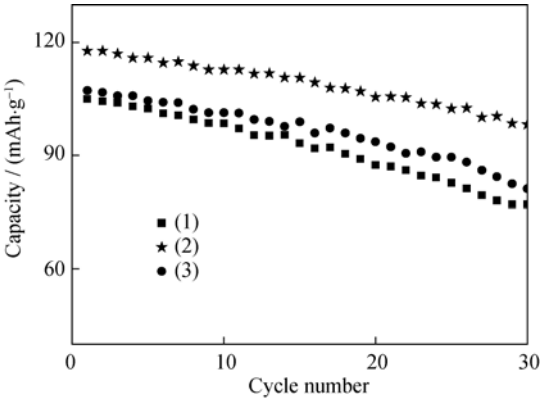

Fig. 6 Cycling performance of $LiMnPO_4$/C samples sintered at different temperatures
(1) 500 °C; (2) 600 °C; (3) 700 °C

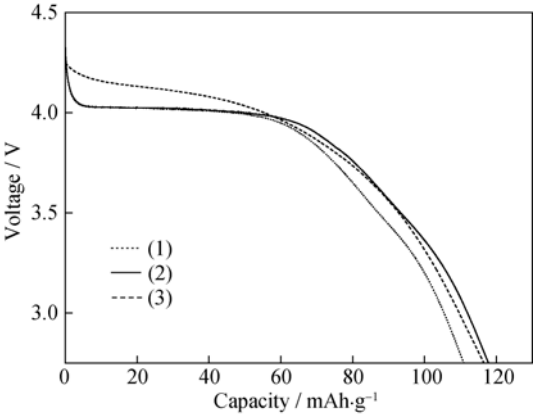

Fig. 7 Initial discharge curves of $LiMnPO_4$/C samples synthesized with different carbon sources
(1) Oxalic acid; (2) Citric acid; (3) Sucrose

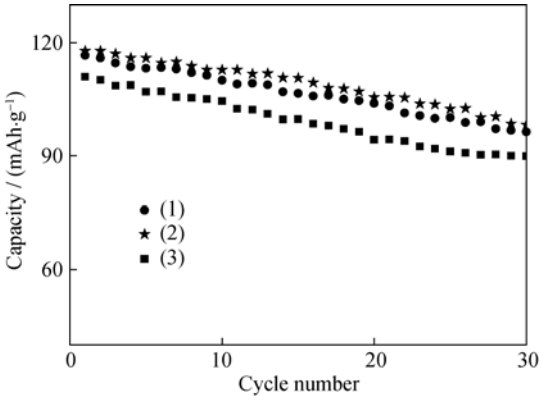

Fig. 8 Cycling performance of $LiMnPO_4$/C samples synthesized with different carbon sources
(1) Oxalic acid; (2) Citric acid; (3) Sucrose

The EIS in the fully charged and discharged state was used to evaluate the lithium ion diffusion coefficient in $LiMnPO_4$/C with different carbon sources. It is obvious that each Nyquist plot is composed of two semicircles in the high frequency and medium frequency region, and a straight line in low frequency region in Figs. 9 and 10. A semicircle is observed to center on the real axis at the high frequency range. In the low frequency range, a straight line with an angle of 45° to the real axis corresponds to the Warburg impedance. The high frequency semicircle is related to the charge-transfer resistance (R_{ct}) and the double-layer capacitance. The low frequency tails result from the diffusion of lithium ions in the bulk active mass. The R_{ct} shows a greater dependence on the lithium insertion and extraction levels. Comparing the diameter of the semicircle of the above, it can be found that citric acid coating (Fig. 9(2) and Fig. 10(2)) shows lower R_{ct} value than the others, which increases the electronic conductivity and improve the Li^+ kinetic behavior. Combined with results of SEM, $LiMnPO_4$/C samples with agglomeration perform the higher R_{ct} value because of the poor lithium diffusion.

The cyclic voltammogram measurements were performed on $LiMnPO_4$/C with citric acid to characterize its electrochemical reactions. Figure 11 shows the cyclic voltammogram curves of $LiMnPO_4$/C. The positions of reduction and oxidation peak are located at 3.916 and 4.406 V. The difference between reduction and oxidation peak is 0.49 V.

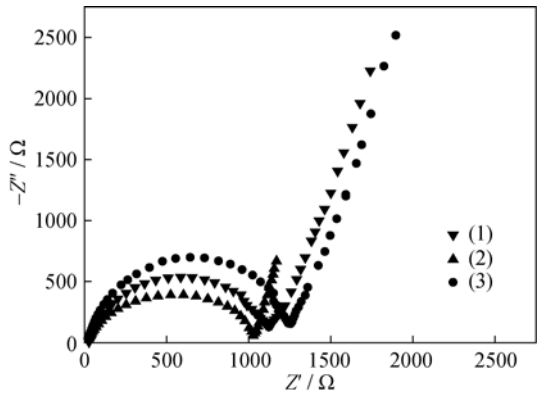

Fig. 9 Nyquist plots of $LiMnPO_4$/C samples with different carbon sources (discharge)
(1) Oxalic acid; (2) Citric acid; (3) Sucrose

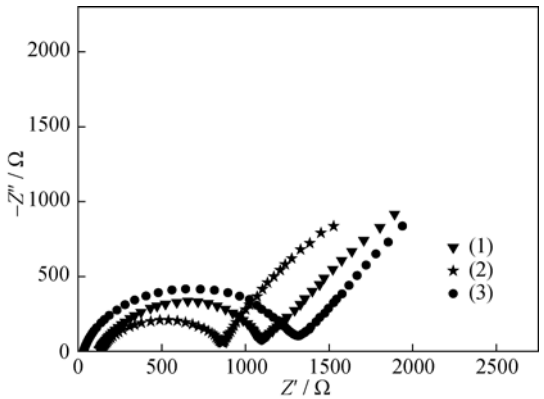

Fig. 10 Nyquist plots of $LiMnPO_4$/C samples with different carbon sources (charge)
(1) Oxalic acid; (2) Citric acid; (3) Sucrose

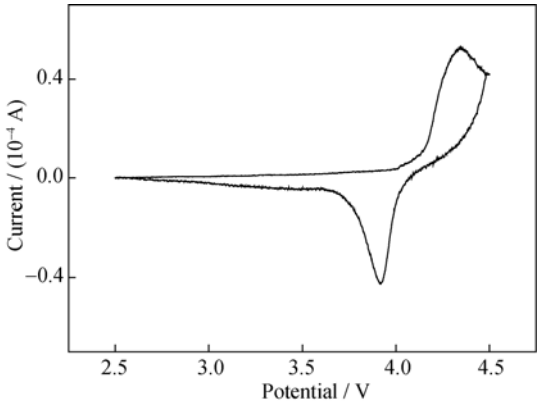

Fig. 11 Cyclic voltammogram curves of $LiMnPO_4$/C

4 Conclusion

Different carbon sources were used to synthesize the $LiMnPO_4$/C. The results of XRD present that pure olivine $LiMnPO_4$/C is obtained by all these carbon sources. With citric acid as carbon source, the $LiMnPO_4$/C synthesized at 600 °C for 20 h has appropriate particle size, while the particle diameter is well-distributed. The decomposition effect of citric acid in the sintering process is attributed to controlling the particle size of $LiMnPO_4$/C. Therefore, it shows the best discharge capacity of 117.8 $mAh \cdot g^{-1}$ at 0.05 C and the retention capacity of 98.2 $mAh \cdot g^{-1}$ over 30 cycles. The EIS shows the lower R_{ct} value than others in charge and discharge state. In conclusion, the conductivity and reversibility of $LiMnPO_4$/C are commendably enhanced, resulting from using citric acid as carbon source.

Acknowledgements

This project was financially supported by Natural Science of Guangxi (No.0991025); Program for Excellent Talents in Guangxi Higher Education Institutions (GuiJiaoRen[No. 2010]65); National Natural Science Foundation of China (No. 51164007); Innovation Project of Guangxi Graduate Education; Educational Commission of Guangxi (No. 201101ZD008); the Important National Science & Technology Specific (No. 2008ZX07317-02-03E), the Key Science Research of Ministry of Education of the Pepople's Republic of China (GuiKeGong0092008) and the Provincial Natural Science Foundation of Guangxi.

References

[1] Morgan D., Van A.D.V., and Ceder G., Li conductivity in Li_xMPO_4 (M=Mn, Fe, Co, Ni) olivine materials, *Eletrochem. Solid-State Lett*., 2004, **7** (11): 30.

[2] Ouyang C.Y., Shi S.Q., Wang Z.X., Huang X.J., and Chen L.Q., First-principles study of Li ion diffusion in $LiFePO_4$, *Phys. Rev*., 2004, **69** (10): 104303.

[3] Islam M.S., Driscoll D.J., Fisher C.A.J., and Slater P.R., Atomic-scale investigation of defects, dopants, and lithium transport in the $LiFePO_4$ olivine-type battery material, *Chem. Mater*., 2005, **17** (20): 5085.

[4] Yonemura M., Yamada A., Takei Y., Sonoyama N., and Kanno R., Comparative kinetic study of olivine Li_xMPO_4 (M = Fe, Mn), *J. Electrochem. Soc*., 2004, **151** (9): 1352.

[5] Fang H.S., Pan Z.Y., Li L.P., Yang Y., Yan G.F., Li G.S., and Wei S.Q., The possibility of manganese disorder in $LiMnPO_4$ and its effect on the electrochemical activity, *Electrochem. Commun*., 2008, **10** (7): 1071.

[6] Yamada A., Kudo Y., and Liu K.Y., Optimized $LiFePO_4$ for lithium battery cathodes, *J. Electrochem. Soc*., 2001, **148** (3): 1153.

[7] Wang Y.R., Yang Y.F., Yang Y.B., and Shao H.X., Enhanced electrochemical performance of unique morphological cathode material prepared by solvothermal method, *Solid State Commun*., 2010, **150** (1-2): 81.

[8] Kwon N.-H., Drezen T., Exnar I., Teerlinck I., Isono M., and Grätzel M., Enhanced electrochemical performance of mesoparticulate $LiMnPO_4$ for lithium ion batteries, *Electrochem. Solid-State Lett*., 2006, **9** (6): 277.

[9] Delacourt C., Laffont L., Bouchet R., Wurm C., Leriche J.-B., Morcrette M., Tarascon J.-M., and Masquelier C., Size effects on carbon-free $LiFePO_4$ powders, *J. Electrochem. Soc*., 2005, **152** (7): 913.

[10] Herle P.S., Ellis B., Coombs N., and Nazar L.F., Nano-network electronic conduction in iron and nickel olivine phosphates, *Nat. Mater*., 2004, **3**: 147.

[11] Liu M.Z., Guo X.Y., Synthesis and performance of $Li_3V_2(PO_4)_3$/C composites as cathode materials, *Rare Metals*., 2008, **27** (6): 571.

[12] Huang H., Yin S.C., and Nazar L.F., Approaching theoretical capacity of $LiFePO_4$ at room temperature at high rates, *Eletrochem. Solid-State Lett*., 2001, **4** (10): 170.

[13] Murugan A.V., Muraliganth T., and Manthiram A., One-pot microwave-hydrothermal synthesis and characterization of carbon-coated $LiMPO_4$ (M= Mn, Fe, and Co) cathodes, *J. Electrochem. Soc*., 2009, **156** (2): 79.

[14] Zhang Y., Sun C.S., and Zhou Z., Sol–gel preparation and electrochemical performances of $LiFe_{1/3}Mn_{1/3}Co_{1/3}PO_4$/C composites with core–shell nanostructure, *Electrochem. Commun*., 2009, **11** (2): 1183.

[15] Mi C.H., Zhao X.B., Cao G.S., and Tu J.P., J. In situ synthesis and properties of carbon-coated $LiFePO_4$ as Li-ion battery cathodes, *Electrochem. Soc*., 2005, **152** (3): 483.

[16] Myung S.T., Komaba S., Hirosaki N., Yashiro H., and Kumagai N., Hydrothermal synthesis of layered $Li[Ni_{1/3}Co_{1/3}Mn_{1/3}]O_2$ as positive electrode material for lithium secondary battery. *Electrochim. Acta*, 2005, **49** (24): 4213.

[17] Huang H., Yin S.C., and Nazar L.F., Approaching theoretical capacity of $LiFePO_4$ at room temperature at high rates, *Electrochem. Solid-State Lett*., 2001, **4** (10): 170.